ISSN 0018-1439, High Energy Chemistry, 2024, Vol. 58, Suppl. 4, pp. S491–S495. © Pleiades Publishing, Ltd., 2024.

Phase Transformations and Kinetics Peculiarities on Hydrogen Desorption by Composites Based in Magnesium–Nickel Eutectic Alloy

P. V. Fursikov[a], *, V. N. Fokin[a], E. E. Fokina[a], A. A. Arbuzov[a], S. A. Mozhzhuhin[a], and B. P. Tarasov[a]

[a] *Federal Research Center of Problems of Chemical Physics and Medicinal Chemistry, Russian Academy of Sciences, Chernogolovka, Moscow oblast, 142432 Russia*

**e-mail: fpv@icp.ac.ru*

Received September 12, 2024; revised September 12, 2024; accepted September 20, 2024

Abstract—The evolution of the phase contents and kinetic characteristics of hydrogen desorption processes by composites based on the eutectic alloy Mg89Ni11, including those with additives of graphene-like material (GLM), obtained by reactive ball-milling in hydrogen, were studied using the in situ high-temperature X-ray diffraction technique, volumetric measurements on a Sieverts setup, and approximation of the registered kinetic curves by Avrami–Erofeev equation. It was shown that at the initial stage of desorption processes at 300–360°C and 0–1 atm. H_2, the decomposition of the magnesium dihydride phase makes the main contribution to the amount of hydrogen released from the composites. The addition of GLM has a positive effect on the kinetics of hydrogen desorption processes, concurring with that of the heat-conducting phase $Mg_2NiH_{\leq 0.3}$, which is also present in the composite. It was found that the apparent activation energy for the hydrogen desorption by composites is within a range of 125–140 kJ/mol H_2. The correlation of the obtained values with the results of both experimental studies and quantum-chemical calculations obtained in the study of other magnesium systems is discussed.

Keywords: magnesium alloys, metal hydride, composite, phase composition, kinetics

DOI: 10.1134/S001814392470156X

THEORETICAL ANALYSIS

One of the most promising materials for reversible hydrogen storage is magnesium due to the high hydrogen content in the dihydride MgH_2 (7.6 wt %), low cost and environmental friendliness [1–3]. However, the wide use of individual magnesium is hindered by the high enthalpy of formation of the MgH_2 phase (75 kJ/mole H_2), poor thermal conductivity of MgH_2 and low rate of hydrogen sorption-desorption in magnesium, which is caused by the high energy barrier (about 100 kJ/mole H_2) of dissociation of H_2 molecules on the metal surface and slow diffusion of H atoms in the MgH_2 phase (at 300°C the diffusion coefficient is about 10^{-18} m^2/s) [4].

It has been commonly known that a significant improvement of the hydrogen sorption properties of magnesium materials can be achieved by forming powder composites based on Mg, in which: (1) the grains of hydride-forming phases in the composite particles have submicro- and nanometer sizes [1], and (2) the composite contains additives that catalyze the dissociation of H_2 molecules on the surface of hydride-forming phases and simultaneously provide good heat exchange in powder composites [5]. It has also been reported elsewhere that another promising method for obtaining such a material for hydrogen storage is to form a powder composite based on a eutectic magnesium-nickel alloy (containing two phases: Mg and Mg_2Ni) with a highly dispersed microstructure in a mixture with carbonaceous graphene-like material (GLM) additives [5].

Various intermetallic compounds containing Ni, such as $LaNi_5$ and also Mg_2Ni have been widely reported [6–8] to accelerate the reaction between the Mg phase and hydrogen. This is due to the fact that these intermetallics, which have catalytic centers on the surface that promote the dissociation of H_2 molecules, provide the H atoms transport across the interface between the active phase of the intermetallic compound and the magnesium phase. Carbonaceous GLM due to its high specific surface area more than 600 m^2/g and extended structure [5] enhances heat transfer in the powder composite material.

In our previous study [9] it was shown that the microstructural characteristics of composites based on the eutectic alloy $Mg_{89}Ni_{11}$, in particular, the grain sizes of the Mg and Mg_2Ni phases and their mutual spatial arrangement in the composite particles, con-

tribute to the improvement of their hydrogen sorption characteristics. Using transmission electron microscopy and selected area electron diffraction techniques, it was shown that these topological features of the microstructure of the composites are preserved in the processes of hydrogen sorption-desorption.

The aim of the present study, being a continuation of [9], is to investigate in situ changes in the phase contents of the hydrogenated composites based on $Mg_{89}Ni_{11}$ during hydrogen desorption, as well as the kinetics of these processes.

EXPERIMENTAL

The procedure for preparing hydrogenated composites based on the eutectic Mg–Ni alloy with the elemental composition $Mg_{89}Ni_{11}$ with the addition of 10 wt % graphene-like material has been described in detail in our previous paper [9].

The prepared composite samples were subjected to 7 hydrogen desorption-absorption cycles, carried out using a Sieverts laboratory setup. Hydrogen absorption was performed at 300°C and 10 atm H_2 for 30 min, desorption at 350°C and 1 atm H_2 for 30 min. After completion of the desorption-absorption cycles, the reactor with the sample was cooled to room temperature for about 3 h at a hydrogen pressure in the system of 10 atm.

The evolution of the phase contents of hydrogenated composites during hydrogen desorption at temperatures of 300–350°C was studied by X-ray diffraction performed in situ on a Thermo Scientific ARL X'TRA Bragg–Brentano CuK_α powder diffractometer equipped with a special high-temperature chamber. A thin layer of powder sample was placed on a tungsten substrate heated to the required temperature at a rate of 300°C/min. The substrate temperature was additionally controlled by the position of the diffraction peak (110) of tungsten, for which the coefficient of thermal expansion is tabulated. The XRD patterns were recorded in a vacuum of no worse than 3.1×10^{-4} mbar, within the 2θ range 19°–33° with a step of 0.05°. The choice of the 2θ range is due to the fact that, taking into account XRD peaks shift due to the thermal expansion, it simultaneously contains intense peaks corresponding to all four phases,—Mg (100), α-MgH_2 (110), Mg_2Ni ($Mg_2NiH_{\leq 0.3}$) (100, 003, 101) and ht-Mg_2NiH_4 (111),—and within this range none of the peaks corresponding to different phases overlap. The exposure time was 1 s that corresponds to the recording time of one XRD pattern 2 min 49 s. The time for positioning the detector in the initial position was 5 s. A set of 22 sequentially recorded XRD patterns was analyzed, in which the first one was recorded at room temperature, the second one started immediately after after the completion of the heating of the substrate and the last one was also recorded at room temperature after cooling the substrate.

The XRD patterns of the composites are characterized by a high level of background and noise; in addition, due to the short detector positioning time and the narrow recording interval in the in situ mode, their full-profile approximation is not reasonable. Therefore, the change in the content of each of the phases was estimated by the change in the integral intensities of the corresponding individual XRD peaks (or the group of peaks for the phase of hydrogen solid solution in Mg_2Ni) which were determined using the CMPR software package [10].

The kinetics of hydrogen desorption processes were studied using a Sieverts laboratory setup in the temperature range of 340–360°C and a hydrogen pressure of 1 atm, as described elsewhere in details [1].

RESIULTS AND DISCUSSION

According to the data of XRD phase analysis carried out at room temperature [9], the hydrogenated composites predominantly contain two crystalline phases: α-MgH_2 (rutile structural type; space group $P4_2/mnm$, no. 136) and pseudo-high-temperature hydride Mg_2NiH_4 (pseudo-ht-Mg_2NiH_4) with a disordered cubic structure (space group $Fm\bar{3}m$, № 225). A small amount of the phase of H solid solution in the intermetallic compound $Mg_2NiH_{\leq 0.3}$ (space group $P6_222$, no. 180) is also present, since under the applied hydrogenation conditions used (10 atm H_2, 300°C) the Mg_2Ni phase is not completely hydrogenated, which is caused by the fact that the specified pressure value practically coincides with the pressure of the sorption plateau in the H_2–Mg_2Ni system [11].

The presence of pseudo-high-temperature hydride Mg_2NiH_4 at room temperature is due to the fact that the synthesis of the phase of low-temperature hydride Mg_2NiH_4 requires special conditions. However, since the phase transition temperature of 245°C [12] of the low-temperature phase into the high-temperature cubic phase is significantly lower than the values at which the studies of sorption/desorption processes were carried out in the present study (300–360°C), then further, when discussing the results, the Mg_2NiH_4 phase will be referred to as the high-temperature hydride with the cubic structure, ht-Mg_2NiH_4.

The data on the evolution of the phase contents of the hydrogenated composites during hydrogen desorption evidences (Fig. 1 shows, for example, the change in the content of each phase over time during dehydrogenation at T = 350°C) that a significant decrease in the content of the α-MgH_2 phase occurs already within an initial stage of the process. Taking into account that the fully hydrogenated $Mg_{89}Ni_{11}$ alloy respectively contains 75.3 mol % and 24.7 mol % of hydrogen in the magnesium dihydride phase and the intermetallic hydride phase, it follows from the

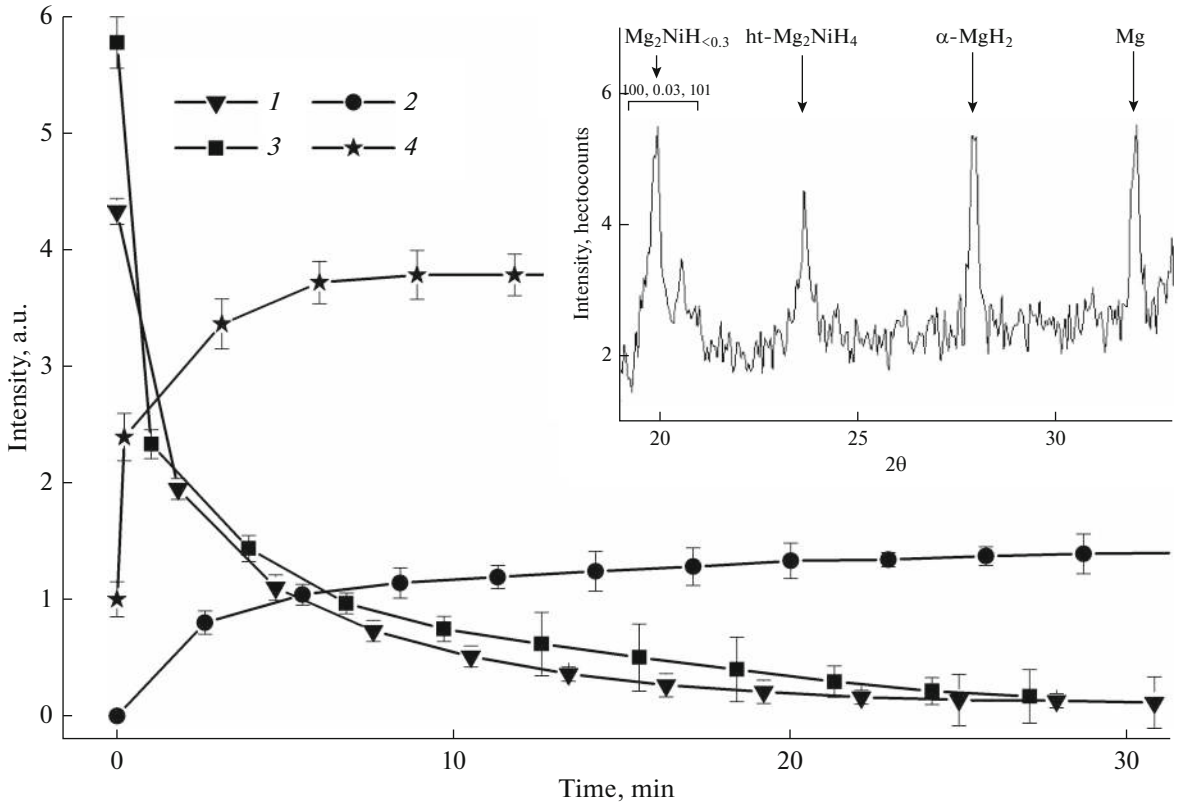

Fig. 1. Integral intensities *vs* time of the XRD peaks of the crystalline phases during dehydrogenation of the composite without GLM additives at 310°C. (*1*) α-MgH_2, (*2*) Mg, (*3*) ht-Mg_2NiH_4, (*4*) Mg_2Ni ($Mg_2NiH_{\leq 0.3}$) The inset shows an intermediate XRD pattern recorded in situ.

data obtained that within the initial stage of hydrogen desorption, the main proportion of the released hydrogen corresponds to that contained in the magnesium dihydride phase.

It is noteworthy that the absence of a strict correlation between the decrease in the peak intensities of MgH_2 and Mg_2NiH_4 and the corresponding increase in the peak intensities of Mg and Mg_2Ni, especially at later times of the dehydrogenation, may be due to the fact that (1) the intensity of a single XRD peak in our case does not unambiguously represents the content of the corresponding phase and (2) the Mg and Mg_2Ni phases formed during dehydrogenation of the composite may partially have a low crystallinity degree and, therefore, make an incomplete contribution to the intensity of the XRD peaks.

Figures 2a and 2b show the hydrogen desorption curves from the hydrogenated composites for three different temperatures of 340, 350, and 360°C. Comparison of the corresponding curves in Figs. 2a and 2b indicates some enhancement of the hydrogen desorption rate for the composite with GLM additives.

This is consistent with the data obtained earlier in our previous study [1], where it was noted that the heat-conducting GLM additive had a positive effect on the rate of hydrogen sorption and desorption due to enhanced heat transfer in the powder sample. However, in the present case of the composite based on the $Mg_{89}Ni_{11}$ alloy, the increase in hydrogen desorption rate is not as significant as in the mentioned study [1], where GLM additives significantly accelerated dehydrogenation and re-hydrogenation of magnesium hydride prepared by reactive ball milling under hydrogen.

As follows from the in situ XRD data, during the entire period of time while the poorly heat-conducting phase of magnesium dihydride MgH_2 is present in the composite, the phase of hydrogen solid solution in the intermetallic compound $Mg_2NiH_{\leq 0.3}$ is also present there. It has been known that the latter phase is an effective catalyst for the hydrogenation of Mg and the dehydrogenation of MgH_2 [13]. In addition, as follows from the data reported in [14], at 300°C $Mg_2NiH_{\leq 0.3}$ exhibits thermal conductivity significantly exceeding that of the hydride phase Mg_2NiH_4, which, as follows from the data of the same study [14], is a good heat conductor only at temperatures below 200°C. Thus, we believe that during hydrogen desorption under the specified experimental conditions, the rate of H desorption and heat transfer in the hydrogenated Mg–Ni based powder are increased due to the presence of

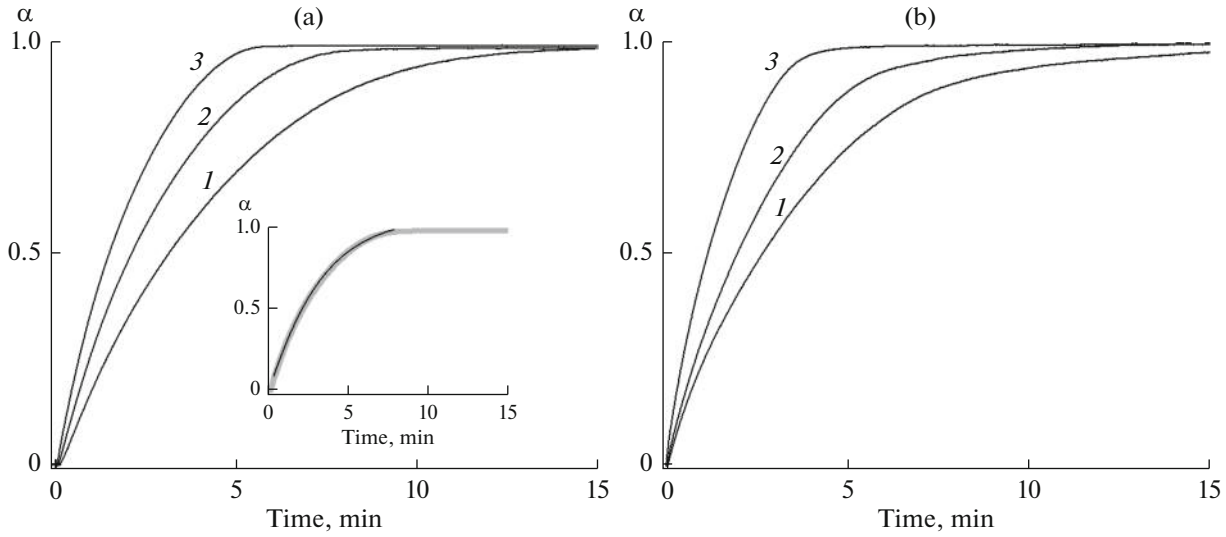

Fig. 2. Hydrogen desorption curves during dehydrogenation of composites without (a) and with (b) GLM additives at 340 (*1*), 350 (*2*), and 360°C (*3*). The inset shows an example of approximation of the initial part of the curves.

the $Mg_2NiH_{\leq 0.3}$ phase in the composite, which to somewhat extent levels the enhancement in the hydrogen desorption rate caused by the GLM additives. At the same time, the data obtained confirm the role of GLM in improving the cyclic stability of Mg-based nanostructured hydrides by preventing sintering of their powder particles at high temperatures [1, 5].

The approximation of the desorption curves in Figs. 2a and 2b using the Avrami–Erofeev (A–E) equation shows that the curves are well fitted by the one-component A–E equation $\ln(1 - \alpha) = -(kt)^n$ (α—reacted fraction, t—time, k—rate constant, n—the Avrami parameter) within an initial time interval of the hydrogen desorption processes. The inset to Fig. 2a shows an example of such an approximation for hydrogen desorption from the composite without GLM additives at 350°C. It is evident that the one-component A-E equation well describes the kinetics of hydrogen desorption from the sample within the initial time interval of up to 7 min. The fitting of desorption curves at three different temperature values of 340, 350, and 360°C gives respective values of the rate constants k of 0.200(1), 0.311(1), and 0.449(1) min^{-1}.

It follows from the above discussion of the data on the evolution of the phase contents of the composites, that the initial parts of the hydrogen desorption curves predominantly correspond to the decomposition of the magnesium dihydride phase. The use of the Arrhenius equation ($\ln k = -E_a/RT + \ln A$, where E_a is the apparent activation energy, A is the pre-exponential factor) gives a value of 131 ± 6 kJ/mol H_2 for the apparent activation energy of the reaction of decomposition of the MgH_2 phase in the composite without GLM additives. Similarly, for its counterpart with GLM additives, $E_a = 130 \pm 20$ kJ/mol H_2.

These values of the apparent activation energy, within the error limits, are in a good agreement with the results of experimental studies and quantum-chemical calculations obtained for other magnesium systems.

In the study mentioned above [1] the apparent activation energy of the dehydrogenation reaction was reported as 127 ± 1 kJ/mol H_2 for a composite of magnesium hydride with 10 wt % catalytic additives of Ni/GLM, and nickel nanoparticles (2–15 nm) were deposited in an amount of 25 wt % of the additive.

The authors of theoretical studies [15, 16], using quantum-chemical calculations of the elementary catalytic cycle of hydrogenation of the homonuclear cluster Mg_{18} in comparison with the doped one $Mg_{17}Ni$, reported that the chemisorption barrier for the reaction $Mg_{18} + H_2 \rightarrow Mg_{18}H_2$ is 130 kJ/mol H_2, and the barrier decreased by approximately an order of magnitude for the doped cluster. In the latter case, the limiting stage of the hydrogenation reaction of $Mg_{17}Ni$ is the "cleaning" of the dopant with an energy barrier of 50–65 kJ/mol H_2.

In a later study [17], quantum-chemical calculations were performed for another magnesium object, the Mg(0001) surface doped with a double heteroatomic catalytic center Ni–Co. Although, unlike the studies mentioned above [15, 16], the authors of [17] did not consider each stage of the hydrogenation process separately, they found that the energy barrier of the hydrogenation reaction has a similar value of 59 kJ/mol H_2.

The experimentally determined value of the apparent activation energy of the dehydrogenation of Mg–Ni based bulk composites, within the error limits, agrees well with the sum of the enthalpy of the forma-

tion of the MgH_2 phase 75 kJ/mol H_2 and the energy barrier of the hydrogenation reaction of Ni-doped magnesium model systems of the subnano- and atomic scale.

CONCLUSIONS

At 300–360°C and 0–1 atm H_2, hydrogen desorption from hydrogenated composites based on $Mg_{89}Ni_{11}$ eutectic alloy occurs predominantly in the kinetic mode (the apparent activation energy is within the range of 125–140 kJ/mol H_2) and that the rate-limiting stage of the process is the decomposition reaction of the α-MgH_2 phase. The addition of GLM has a positive effect on the kinetics of hydrogen desorption processes, even in the presence of the heat-conducting phase $Mg_2NiH_{\leq 0.3}$ in the composite, although this effect is not as pronounced as in the case of other magnesium-based systems that do not contain intermetallic phases [1].

Not only the qualitative but also the quantitative correspondence between the results of experimental studies of bulk magnesium systems and quantum-chemical calculations of atomic- and subnano-sized objects confirms the assumption reported in [16] that the energy barrier of the hydrogenation reaction of a doped magnesium cluster defined in quantum-chemical calculations would have a similar value for much larger magnesium based systems.

FUNDING

The work was carried out under the support from the Ministry of Science and Higher Education of the Russian Federation (Megagrant, Agreement no. 075-15-2022-1126, signed on July 1, 2022).

CONFLICT OF INTEREST

The authors of this work declare that they have no conflicts of interest.

REFERENCES

1. Tarasov, B.P., Arbuzov, A.A., Mozhzhuhin, S.A., et al., *Int. J. Hydrogen Energy*, 2019, vol. 44, p. 29212.
2. Osman, A.I., Ayati, A., Farrokhi, M., et al., *J. Energy Storage*, 2024, vol. 95, p. 112376.
3. Hong, H., Guo, H., Cui, Z., et al., *Int. J. Hydrogen Energy*, 2024, vol. 78, p. 793.
4. Fursikov, P.V., Tarasov, B.P., *Russ. Chem. Bull.*, 2018, vol. 67, p. 193.
5. Tarasov, B.P., Arbuzov, A.A., Volodin, A.A., et al., *J. Alloys Compd.*, 2022, vol. 896, p. 162881.
6. Fursikov, P.V., Borisov, D.N., Tarasov B.P., *Russ. Chem. Bull.*, 2011, vol. 60, p. 1848.
7. Yartys, V.A., Lototskyy, M.V., Akiba, E, et al., *Int. J. Hydrogen Energy*, 2019, vol. 44, p. 7809.
8. Grigorova, E., Tzvetkov, P., Todorova, S, Markov P, Spassov T., *Materials*, 2021, vol. 14, p. 1936. https://doi.org/10.3390/ma14081936
9. Fursikov, P.V., Fokin, V.N., Fokina, E.E., et al., *High Energy Chem.*, 2023, vol. 57, Suppl. 2, p. S50.
10. Toby, B.H., *J. Appl. Crystallogr.*, 2005, vol. 38, p. 1040.
11. Schefer, J., Fischer, P., Hälg, W., et al., *J. Less-Common Met.*, 1980, vol. 74, p. 65.
12. Senegas, J., Mikou, A., Pezat, M., et al., *J. Solid State Chem.*, 1984, vol. 52, p. 1.
13. Mazzaro, R. and Pasquini, L., *J. Alloys Compd.*, 2022, vol. 911, p. 165014.
14. Blomqvist, H. and Noréus, D., *J. Appl. Phys.*, 2022, vol. 91, p. 5141.
15. Charkin, O.P. and Maltsev, A.P., *J. Phys. Chem. A*, 2021, vol. 125, p. 2308.
16. Maltsev, A.P. and Charkin, O.P., *Russ. J. Inorg. Chem.*, 2021, vol. 66, p. 1860.
17. Liu, B., Liang, S., Huang, H., et al., *J. Energy Storage*, 2024, vol. 94, p. 112410.